Received: 15 March 2021 | Revised: 17 August 2021 | Accepted: 18 August 2021

DOI: 10.1111/pce.14196

ORIGINAL ARTICLE

Plant, Cell & Environment WILEY

Cytosolic proline is required for basal freezing tolerance in Arabidopsis

Imke I. Hoermiller[1] | Dietmar Funck[2] | Lilli Schönewolf[1] | Henrik May[1] | Arnd G. Heyer[1]

[1]Department of Plant Biotechnology, University of Stuttgart, Institute of Biomaterials & Biomolecular Systems, Stuttgart, Germany

[2]Department of Biology, University of Konstanz, Constance, Germany

Correspondence
Arnd G. Heyer, Department of Plant Biotechnology, University of Stuttgart, Institute of Biomaterials & Biomolecular Systems, Stuttgart 70569, Germany.
Email: arnd.heyer@bio.uni-stuttgart.de

Funding information
Deutsche Forschungsgemeinschaft, Grant/Award Number: HE-3087/10-2

Abstract

The amino acid proline accumulates in many plant species under abiotic stress conditions, and various protective functions have been proposed. During cold stress, however, proline content in *Arabidopsis thaliana* does not correlate with freezing tolerance. Freezing sensitivity of a starchless *plastidic phosphoglucomutase* mutant (*pgm*) indicated that localization of proline in the cytosol might stabilize the plasma membrane during freeze–thaw events. Here, we show that re-allocation of proline from cytosol to vacuole was similar in the *pyrroline-5-carboxylate synthase 2–1* (*p5cs2–1*) mutant and the *pgm* mutant and caused similar reduction of basal freezing tolerance. In contrast, the *starch excess 1–1* mutant (*sex1-1*) had even lower freezing tolerance than *pgm* but did not affect sub-cellular localization of proline. Freezing sensitivity of *sex1-1* mutants affected primarily the photosynthetic electron transport and was enhanced in a *sex1-1*::*p5cs2–1* double mutant. These findings indicate that several independent factors determine basal freezing tolerance. In a *pgm*::*p5cs2–1* double mutant, freezing sensitivity and proline allocation to the vacuole were the same as in the parental lines, indicating that the lack of cytosolic proline was the common cause of reduced basal freezing tolerance in both mutants. We conclude that cytosolic proline is an important factor in freezing tolerance of non-acclimated plants.

KEYWORDS
Arabidopsis, freezing, pgm, proline, pyrroline-5-carboxylate synthase, sex1, starch

1 | INTRODUCTION

Accumulation of proline (Pro) is a common physiological response of many plants to biotic and abiotic stress and is believed to play an adaptive role in plant stress tolerance (Meena et al., 2019; Verbruggen & Hermans, 2008). Recently, evidence has been presented that Pro-stimulated signalling prevents chlorophyll degradation under water stress (Altuntaş, Demiralay, Sezgin Muslu, & Terzi, 2020), and there are reports that Pro protects enzymes by modulating electrostatic interactions and stabilizing the tertiary structure (Govrin, Obstbaum, & Sivan, 2019; Rydeen, Brustad, & Pielak, 2018). Additionally, there is evidence that Pro activates the antioxidative defense, either directly or through ROS signalling originating from mitochondrial Pro degradation (Szabados & Savouré, 2010). However, several studies have challenged the assumption of a protective function of Pro accumulation under osmotic stress (Maggio et al., 2002; Székely et al., 2008; Xin & Browse, 2000).

A role of Pro in non-acclimated tolerance of plants, that is, before any stress treatment, has rarely been considered, especially because

the rather low concentrations seem to preclude a role in osmoregulation (Forlani, Trovato, Funck, & Signorelli, 2019). The lack of correlation of Pro levels with stress tolerance stimulated the hypothesis that not the total amount of Pro but the rate of its turnover might be important for cellular protection (Sharma, Joji Grace Villamor, & Verslues, 2011; Szabados & Savouré, 2010). In contrast, the impact of sub-cellular localization of Pro for its role in stress tolerance has not yet been evaluated, although allocation to specific sub-cellular compartments will greatly influence the actual concentration in these compartments (Büssis & Heineke, 1998).

Pro synthesis and degradation are multi-compartment processes involving primarily cytosol and mitochondria (Funck, Baumgarten, Stift, von Wirén, & Schönemann, 2020). In Arabidopsis, Pro synthesis occurs predominantly in the cytosol, where pyrroline-5-carboxylate synthase (P5CS) converts glutamate to glutamate-5-semialdehyde, which is in spontaneous equilibrium with pyrroline-5-carboxylate. Pyrroline-5-carboxylate is further reduced to Pro by pyrroline-5-carboxylate reductase (Funck, Winter, Baumgarten, & Forlani, 2012; Mattioli et al., 2018). P5CS is thought to be rate limiting for Pro synthesis, and Arabidopsis has two isoforms of P5CS with different expression patterns and functions: P5CS2 is the housekeeping enzyme, while P5CS1 is considered to mediate stress-induced Pro accumulation (Funck et al., 2012; Székely et al., 2008). Degradation of Pro occurs in the mitochondria, where it is oxidized by Pro dehydrogenase (PDH) (Szabados & Savouré, 2010). In animals, Pro can also be synthesized by an alternative pathway from ornithine, which can be converted to glutamate-5-semialdehyde by ornithine-δ-aminotransferase. In plants, the operation of such a pathway is hampered by differential sub-cellular localization of the transferase and the reductase and is controversial (Funck, Stadelhofer, & Koch, 2008; Miller et al., 2009).

In a recent study addressing sub-cellular re-programming of metabolism during cold acclimation, we have shown that the sub-cellular localization of Pro in non-acclimated Arabidopsis plants was influenced by starch metabolism. In the mostly starch-less *pgm* mutant, deficient in plastidic phosphoglucomutase (pPGM), vacuolar Pro was increased, whereas in wild-type plants, Pro was mainly cytosolic (Caspar, Huber, & Somerville, 1985; Hoermiller et al., 2017). This coincided with reduced freezing tolerance of the *pgm* mutant. To determine whether Pro could indeed be involved in freezing tolerance of non-acclimated plants, knockout mutants of the two *P5CS* genes as well as a double mutant of the two isoforms of proline dehydrogenase (*pdh1-1*::*pdh2-1*) were used. Pro content of non-acclimated plants was affected only by the *p5cs2–1* mutation, and this mutant, like *pgm*, showed reduced basal freezing tolerance. We generated *pgm*::*p5cs2–1* double mutants to investigate, whether freezing sensitivity of *pgm* could be causally related to its low cytosolic Pro content. Freezing sensitivity was not further enhanced in the double mutant, indicating the operation of a common mechanism in both single mutants.

In addition, we wondered whether starch over-accumulation would also affect freezing tolerance. The *sex1-1* mutant contains a G1268E substitution in the C-terminal region of the plastidic glucan/water dikinase, R1, (Yu et al., 2001) and thus has a low degree of starch phosphorylation. This leads to slow degradation of starch, resulting in very high starch content of plastids. With respect to starch content, the *sex1-1* mutant is the antipode of *pgm*. However, they are both retarded in growth because both mutants cannot make use of starch as a carbon store during the night (Rasse & Tocquin, 2006). Yano, Nakamura, Yoneyama, and Nishida (2005) reported transiently reduced freezing tolerance of the *sex1-1* mutant after cold acclimation in continuous light. Here we show that for growth in day–night cycles, both, *pgm* and *sex1-1* mutants, are freezing sensitive, but only in the *pgm* mutant, this is related to altered sub-cellular localization of Pro.

2 | MATERIALS AND METHODS

2.1 | Plant material and growth conditions

Arabidopsis thaliana (L.) Heynh. (*Brassicaceae*), accession Col-0, and the following mutants were used in this study: *pgm-1* (At5g51820; NASC ID 210), *sex1-1* (At1g10760, NASC ID N212), *p5cs1–4* (Salk_063517), *p5cs2–1* (GABI452_G01; Funck et al., 2012) and *pdh1-1*::*pdh2-1* (O'Leary, Oh, Lee, & Millar, 2019). Double mutants of *pgm* and *pc5cs2–1* (*p5cs2–1*::*pgm*) and *sex1-1* and *p5cs2–1* (*p5cs2–1*::*sex1-1*) were created by crossing the parental lines. Like *in p5cs2–1* single mutants, homozygous *p5cs2–1* double-mutant embryos were retarded in development when the parent was heterozygous but could be rescued by *in vitro* cultivation of immature seeds in the presence of 1 mM proline, as described in Funck et al. (2012). Double homozygous mutants were confirmed by PCR analysis and showed normal embryo and seed development when grown in a greenhouse under short-day condition. All plants for physiological analysis were grown in soil (*seedling substrate*, Klasmann-Deilmann GmbH, Geeste, Germany) and vermiculite (1:1) in a growth chamber with 8 hr/16 hr light/dark regime (100 μmol m^{-2} s^{-1}; 22°C/16°C) to avoid floral induction and stimulate biomass formation. After 5 weeks, plants were transferred to long day, and a 16 hr/8 hr light/dark regime was applied (100 μmol m^{-2} s^{-1}; 22°C/16°C). The relative humidity was 70%. Plants were watered regularly and fertilized with nitrogen:phosphate:potassium fertilizer 4 and 6 weeks after sowing. Directly before bolting, that is 8 days after transfer to long-day conditions, a set of plants was harvested and another set was shifted to a growth chamber with 16 hr/8 hr light/dark regime at 4°C. A light intensity of 50 μmol m^{-2} s^{-1} at 4°C was chosen to minimize differences in diurnal starch turnover for the ambient and cold temperature treatment in order to reduce effects of different starch levels on sugar metabolism. For metabolite analysis, whole rosettes of six independent biological replicates were sampled at the mid-point of the light period. Samples were immediately frozen in liquid nitrogen, frozen leaves were ground to a fine powder using a MM200 ball mill (Retsch GmbH, Haan, Germany) and stored at −80°C until further use.

2.2 | Physiological analyses

Freezing tolerance was determined using the electrolyte leakage method essentially as described earlier (Knaupp, Mishra, Nedbal, &

Heyer, 2011). Briefly, three fully expanded rosette leaves taken from three individual plants were placed in a glass tube containing 200 µl of distilled water. Twelve tubes were used to constitute one set of samples analyzed for 12 different temperatures. Tubes were transferred to a programmable cooling bath set to −1°C; a control was left on ice during the entire experiment. After 30 min of temperature equilibration at −1°C, ice crystals were added to the tubes to initiate freezing. After another 30 min, the samples were cooled at a rate of 4°C hr^{-1}. Over a temperature range of −1°C to −15°C for non-acclimated plants, and −1°C to −17°C for acclimated plants, the samples were taken sequentially at even intervals from the bath and thawed slowly on ice. After incubation in 6 ml of distilled water over night at 4°C on a shaker, 500 µl of the bathing solution were mixed with 2.5 ml deionized water before measurement of electrical conductivity by an LR 325 electrode coupled to an Inolab 740 system (WTW, Weilheim, Germany). The vessels were then incubated at 95°C for 30 min; conductivity was measured again, and relative damage was expressed as the conductivity ratio before and after boiling of the sample. The temperature of 50% electrolyte leakage ($LT_{50}EL$) was calculated as the temperature causing the half-maximal effect by fitting sigmoidal curves to the leakage values of one sample series using the package 'drc' (Ritz, Baty, Streibig, & Gerhard, 2015) of the R statistical software (R Core Team, 2016).

Fluorescence imaging of detached leaves after freeze–thaw cycles was performed as described in Knaupp et al. (2011). Detached leaves were frozen and thawed in the same manner as leaves used for the electrolyte leakage assays. In four independent experiments, chlorophyll fluorescence data of leaves directly after thawing were compared. Leaves were adapted for 10 min in the dark before measuring the chlorophyll fluorescence with a Handy FluorCam, model FC 1000-H (Photon Systems Instruments, Brno, Czech Republic, www.psi.cz) set at shutter frequency 10 µs, sensitivity 40%, actinic light 30%, saturation pulse 15% and dark red pulse 20%. Fluorescence parameters were averaged over the whole leaf area and the integrated data from leaves frozen to different temperatures were used to calculate $LT_{50}F_V/F_M$ and $LT_{50}\Phi PSII$ values analogous to the $LT_{50}EL$ values derived from the electrolyte leakage measurements.

2.3 | Metabolite analyses

For soluble sugars and starch, pulverized plant material was extracted twice in 400 µl of 80% ethanol at 80°C. Extracts were dried and dissolved in 500 µl of distilled water. Contents of glucose, fructose, sucrose and raffinose were analyzed by high-performance anion exchange chromatography (HPAEC) using a CarboPac PA-1 column on a DX-500 gradient chromatography system coupled with pulsed amperometric detection by a gold electrode (Dionex, Sunnyvale, CA). For starch extraction, residues of the ethanol extraction were solubilized by heating them to 95°C in 0.5 N NaOH for 45 min. After acidification with 1 N acetic acid, the suspension was digested for 2 hr with amyloglucosidase. The glucose content of the supernatant was determined via a coupled enzymatic assay resulting in the oxidation of o-anisidine, which was measured photometrically at 540 nm and used to assess the starch content of the sample.

For a qualitative metabolite profiling by GC/MS analysis, 10 mg of fine tissue powder were extracted in 750 µl methanol plus 5 µl 10 mM ribitol as internal standard. After 15 min at 70°C, samples were centrifuged, the supernatant was transferred to a fresh tube, and the pellet was extracted with 400 µl of water at 95°C for 10 min. After centrifugation, supernatants were combined, and 200 µl of chloroform plus 300 µl of water were added for phase separation. The polar upper phase and the non-polar lower phase were separately dried under vacuum. Both extracts were derivatized by adding 20 µl of pyridine plus 0.8 mg methoxyamine-hydrochloride and incubation at 30°C for 90 min under constant shaking. Then, 80 µl *N*-methyl-*N*-trimethylsilyl-trifluoroacetamide (MSTFA) reagent were added. After 30 min at 50°C, samples were centrifuged, and the supernatant was injected into the GC/MS system. For analysis, a TQ8040 system (Shimadzu, Munich, Germany) was used in Q3 scan mode. The temperature gradient for GC was from 70°C to 330°C with 15° min^{-1}. The injector port was held at 230°C, detector temperature was 280°C. Carrier gas was helium.

2.4 | Non-aqueous fractionation of subcellular compartments

NAF was performed as described (Hoermiller et al., 2017). Approximately, 100–150 mg of freeze-dried leaf tissue was suspended in 10 ml heptane:tetrachlorethylene ($\rho = 1.34$ g cm^{-3}) and sonicated for 5 s with pauses of 15 s over a time course of 12 min (Branson Sonifier 250, output control 4; Branson, USA). The sonicated suspension was passed through a nylon gauze of 30 µm pore size and centrifuged afterwards. The pellet was suspended in heptane:tetrachlorethylene and loaded onto a linear gradient of heptane:tetrachlorethylene ($\rho = 1.34$ g cm^{-3}) to tetrachlorethylene ($\rho = 1.6$ g cm^{-3}). After ultracentrifugation for 3 hr at 4°C at 100,000 g, the gradient was fractionated into nine fractions that were further aliquoted and dried under vacuum. One aliquot was used for marker enzyme determination, another one for metabolite analysis. Activities of alkaline pyrophosphatase as a plastidic marker, UGPase as a cytosolic marker and acid phosphatase as marker for the vacuolar compartment were measured essentially as described (Knaupp et al., 2011). Pro quantification followed the method of Rienth et al. (2014). In brief, aliquots of the fractions from density gradients, equivalent to 2/3 of the original fraction, were extracted for 10 min in 450 µl Tris/HCl, pH 8.0 at 4°C and centrifuged (15,600 g for 15 min). Two hundred microlitre of supernatant were mixed with 250 µl of concentrated formic acid and vortexed for 5 min. Two hundred microlitre of ninhydrin reagent (3% [w/v] ninhydrin in dimethylsulfoxide) were added, the samples heated (100°C for 15 min) and immediately cooled on ice before centrifugation at 15,600 g for 1 min. Absorption at 520 nm was used as a measure of Pro content (Ultraspec 2000 UV/VIS Spectrophotometer, Pharmacia Biotech). A control without ninhydrin was used as reference.

2.5 | Statistical analyses

The R software package, version 3.3.1, was used for statistical analysis (R Core Team, 2016). Because homogeneity of variance was not given in comparisons of non-acclimated and acclimated samples, one-way analysis of variance (ANOVA) in subgroups of either non-acclimated or acclimated samples was applied to test for genotype effects. The effect of cold acclimation was assessed using Welch's *t*-test for unequal variances within a given genotype. Therefore, no general statement on the effect of cold acclimation is made. Tukey's HSD, as implemented in the 'agricolae' package (de Mendiburu, 2016), was used as post hoc test for ANOVA at a significance level of $p < .05$. Data are visualized as bar charts of the mean with standard error of the mean.

Statistical analysis of compartmentation data was performed using the R package 'compositions' (van den Boogaart & Tolosana-Delgado, 2008). Briefly, the *rcomp* function is used to construct a matrix of relative distributions of a metabolite over the three compartments from the measured percentage values. The *ipt* function calculates an isometric planar transform of the dataset, which is analysed for a genotype effect by applying a linear model. If a genotype effect is detected for three compartments, ANOVA is applied to subcompositional fits for two compartments. Because the null hypothesis was rejected for the three-compartment model, acceptance of the null hypothesis in a test for subcompositions marks an effect in the compartment that was left out.

3 | RESULTS

3.1 | Freezing tolerance is reduced in mutants affected in pro or starch metabolism

Two *P5CS* mutants as well as a double mutant of both *PDH* genes, the *pgm* and the *sex1-1* mutant were used to investigate the effect of altered Pro and starch metabolism on freezing tolerance. Under our cultivation conditions, the *p5cs2–1* as well as the two starch metabolism mutants consistently showed growth reduction with *pgm* being the smallest genotype (Figure S1).

Freezing tolerance of Pro metabolism mutants was analysed using the electrolyte leakage method that reports damage to the plasma membrane as a major incidence of freezing injury in plants. The temperature that caused half maximal damage ($LT_{50}EL$) was not different from wild type in *p5cs1–4* mutants, *pdh1-1*::*pdh2-1* double mutants and in cold-acclimated *p5cs2–1* mutants (Figure 1a). However, the basal freezing tolerance of non-acclimated *p5cs2–1* mutants was reduced. As expected, Pro levels were reduced in non-acclimated *p5cs2–1* plants as well as in acclimated *p5cs1–4* mutants when compared to the wild type, while the *pdh1-1*::*pdh2-1* mutant displayed no significant deviation from wild type under either condition (Figure 1b). Thus, the *p5cs2-1* mutant was chosen for further analyses.

To determine whether reduced non-acclimated freezing tolerance of *p5cs2–1* had a similar cause as in the *pgm* mutant, double mutants of *p5cs2–1 and pgm* as well as *sex1-1* plants were created and analysed for freezing tolerance in the non-acclimated and cold acclimated state. All mutants displayed significantly ($p < .05$) reduced freezing tolerance as compared to wild type before cold acclimation (Figure 2). The lowest freezing tolerance in non-acclimated plants was found for *p5cs2–1*::*sex1-1*, followed by *sex1-1*, *pgm*, *p5cs2–1*::*pgm* and *p5cs2–1*, with *pgm* and *p5cs2–1*::*pgm* not deviating from each other. In each individual genotype, cold tolerance increased upon cold acclimation (*t*-test, $p < .05$). The *pgm* and the double-mutant *p5cs2–1*::*pgm* displayed similar freezing tolerance after cold acclimation but differed from *sex1-1* and *p5cs2–1*::*sex1-1* in the non-acclimated state. Acclimation capacity, denoting the difference between $LT_{50}EL$ of acclimated and non-acclimated plants, was −4.7°C in *p5cs2–1* and varied from −3.0°C to −3.3°C in the other genotypes.

3.2 | Metabolite changes during cold exposure at the whole-cell level

Plants cultivated at ambient temperature and harvested in the middle of a 16 hr light period showed the expected genotype effects on starch, sugar and Pro levels. Starch levels were below the detection limit in *pgm* and *p5cs2–1*::*pgm* plants before and after cold

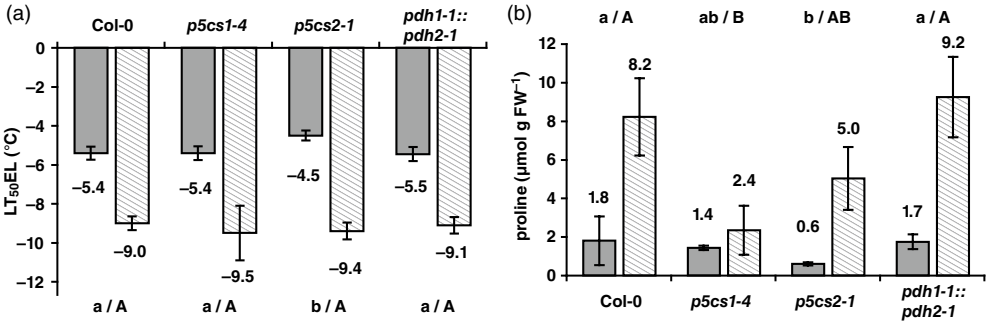

FIGURE 1 Freezing tolerance (a) and Pro content (b) of wild-type and mutants of Pro metabolism grown at ambient temperature (22°C, grey bars) or cold acclimated at 4°C for 1 week (hatched bars). Freezing tolerance is expressed as the temperature, at which 50% of the tissue had suffered membrane damage ($LT_{50}EL$), measured as electrolyte leakage and calculated by non-linear regression for four series of samples per genotype and condition ($n = 4$). Error bars show 95% confidence intervals. Groups that do not share common letters are significantly different ($p < .05$) within one treatment (lowercase for non-acclimated, uppercase for acclimated). Pro content is given as µmol $(g\ FW)^{-1}$ ± standard error of the mean (SEM) ($n = 5$)

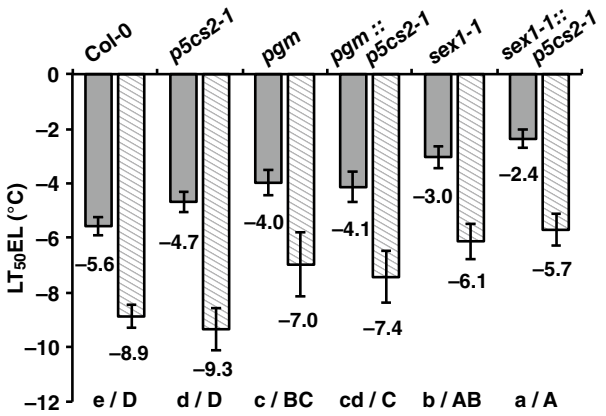

FIGURE 2 Freezing tolerance of the six genotypes Col-0, *p5cs2–1*, *pgm*, *p5cs2–1*::*pgm*, *sex1-1* and *p5cs2–1*::*sex1-1*, expressed as the temperature of half-maximal electrolyte leakage ($LT_{50}EL$) from non-acclimated (grey bars) and cold acclimated (hatched bars) leaves. Values are calculated by non-linear regression for four series of samples per genotype and condition ($n = 4$). Error bars show 95% confidence intervals. Groups that do not share common letters are significantly different ($p < .05$) within one treatment (lowercase for non-acclimated, uppercase for acclimated)

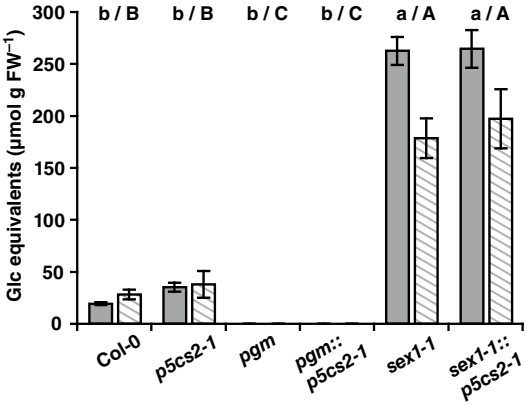

FIGURE 3 Leaf starch content in the six genotypes Col-0, *p5cs2–1*, *pgm*, *p5cs2–1*::*pgm*, *sex1-1* and *p5cs2–1*::*sex1-1* before (grey bars) and after (hatched bars) cold acclimation. Starch content is expressed as µmol glucose equivalents per (g FW). Values are means ± standard error of the mean (SEM) ($n = 5$). Groups that do not share common letters are significantly different ($p < .05$) within one treatment (lowercase for non-acclimated, table of effects: Col-0:80.39; *p5cs2–1*:-64.68; *pgm*: 99.58; *pgm*::*p5cs2–1*: −99.53; *sex1-1*:162.8; *sex1-1*::*p5cs2–1*:164.7; upper case for cold-acclimated, table of effects: Col-0: −33.2 *p5cs2–1*: −22.84; *pgm*: −60.29; *pgm*::*p5cs2–1*:-60.29; *sex1-1*:99.44; *sex1-1*::*p5cs2–1*:112.5)

acclimation, whereas *sex1-1* and *p5cs2–1*::*sex1-1* plants had much higher starch levels than Col-0 and *p5cs2–1*, the latter having slightly higher starch content than wild-type grown at 22°C (Figure 3). Low temperature led to a significant drop in starch content in *sex1-1* and *p5cs2–1*::*sex1-1* (*t*-test, $p < .05$), causing a 32% and 25% reduction, respectively, while starch accumulated 1.5-fold in Col-0 at 4°C (*t*-test, $p < .05$). Hexoses and sucrose levels were elevated in *pgm*, while *sex1-1* did not deviate significantly from wild type (Figure 4). The *p5cs2-1* mutant showed significantly lower hexose content than the wild type, but sucrose and raffinose did not deviate at ambient temperature. At 22°C, loss of P5CS in the double-mutants *p5cs2–1*::*pgm* and *p5cs2–1*::*sex1-1* exhibited divergent effects: in *p5cs2–1*::*pgm*, soluble sugars levels were significantly higher as compared to *pgm* and *p5cs2–1*, but no effect of the double mutation was found for *p5cs2–1*::*sex1-1*.

After 7 days of cold exposure, increased hexose content was observed in each of the genotypes (*t*-test, $p < .05$), except for *p5cs2–1*::*pgm*. Raffinose levels rose in each genotype upon cold exposure (*t*-test, $p < .05$). Most genotypes, except *pgm*, did not significantly deviate from wild type for raffinose and sucrose after cold exposure. The *pgm* mutant was different from all others with significantly higher sucrose levels compared to wild type at ambient temperature but significantly lower at 4°C (Figure 4a–c).

Undirected metabolite profiling of polar extracts from leaf tissue yielded only few metabolites discriminating *sex1-1* mutants from wild-type plants (Figure S2). An outstanding metabolite was maltose, for which, non-acclimated *sex1-1* and *p5cs2–1*::*sex1-1* had much higher content than all other genotypes.

Free Pro levels varied significantly among genotypes (Figure 5). At ambient temperature, the level was more than two-fold higher in Col-0 than in *pgm* and *sex1-1* and more than four-fold higher than in *p5cs2–1* and the double mutants. The Pro content increased 4- to seven-fold in all genotypes upon cold acclimation. However, in the acclimated state, only the genotypes containing the *p5cs2–1* mutation had significantly lower Pro content than Col-0 plants, whereas *pgm* and *sex1-1* differed neither from wild type nor from the *p5cs2–1* mutants. Correlation of Pro levels or hexose content with $LT_{50}EL$ values was detected neither for non-acclimated nor for acclimated plants ($p > .1$).

3.3 | Subcellular compartmentation of pro differs among the genotypes at ambient temperature

Given the lack of correlation of Pro levels with non-acclimated freezing tolerance, we analysed the subcellular distribution of Pro in plants grown at 22°C. Whole rosettes of six independent biological replicates per genotype were used for subcellular fractionation of plastids, cytosol and vacuole (Figure 6). As observed previously (Hoermiller et al., 2017), Pro was tightly associated with the cytosol in Col-0 but not so in *pgm*. Strikingly, the *p5cs2-1* mutant showed the same pattern as *pgm*, with mainly vacuolar instead of cytosolic Pro allocation, and there was no additive effect for the double-mutant *p5cs2–1*::*pgm*. In contrast, Pro distribution of *sex1-1* was similar to Col-0, while being intermediate between the two genotypes in *p5cs2–1*::*sex1-1* double mutants. Considering the high sensitivity to freezing of *sex1-1* and *p5cs2–1*::*sex1-1*, this indicates that there must be additional effects explaining the reduced freezing tolerance in these genotypes.

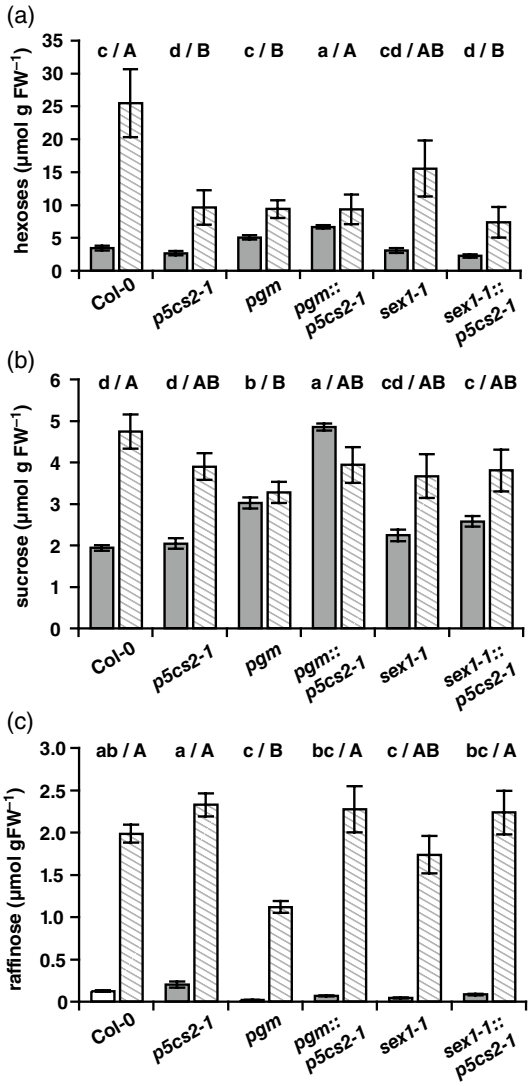

FIGURE 4 Leaf sugar content in the six genotypes Col-0, *p5cs2–1*, *p5cs2–1::pgm*, *sex1-1* and *p5cs2–1::sex1-1* before (grey bars) and after (hatched bars) cold acclimation. (a): hexoses; (b): sucrose; (c): raffinose. Values are means ± standard error of the mean (SEM) ($n = 5$). Groups that do not share common letters are significantly different ($p < .05$) within one treatment (lowercase for non-acclimated, uppercase for cold acclimated)

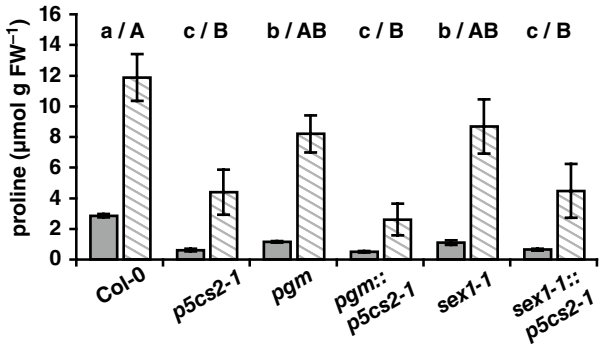

FIGURE 5 Leaf Pro levels in µmol (g FW)$^{-1}$ fresh weight in the six genotypes Col-0, *p5cs2–1*, *pgm*, *p5cs2–1::pgm*, *sex1-1* and *p5cs2–1::sex1-1* before (grey bars) and after (hatched bars) cold acclimation. Values are means ± standard error of the mean (SEM) ($n = 5$). Groups that do not share the same letter (lowercase for non-acclimated, uppercase for acclimated) are significantly different ($p < .05$)

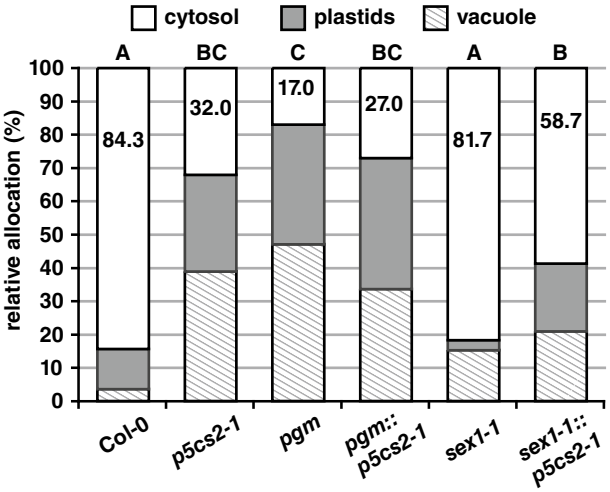

FIGURE 6 Subcellular compartmentation of Pro in the six genotypes Col-0, *p5cs2–1*, *pgm*, *p5cs2–1::pgm*, *sex1-1* and *p5cs2–1::sex1-1* before cold acclimation. Relative allocation of Pro to cytosol, plastid and vacuole was determined by non-aqueous fractionation and calculated with a three-compartment model based on four replicates per genotype ($n = 4$). Different letters above the bars indicate significant differences for cytosolic portion of Pro as calculated form compositional data analysis (see Material and Methods)

3.4 | Photosynthetic electron transport is more sensitive to freezing in *sex1-1* mutants

Given that the *sex1* mutation affects starch phosphorylation and degradability, we wondered whether freezing sensitivity of the *sex1-1* genotype might derive from the plastids. As a sensitive method to analyse freezing damage to plastids, we used chlorophyll fluorescence imaging of leaves subjected to a freeze–thaw event with minimal temperatures in the range of zero to −12°C (non-acclimated) and −17°C (acclimated). The temperature of half-maximal damage was calculated for the maximum quantum yield (F_V/F_M) as a parameter for dark-adapted plants and the steady state quantum yield (ΦPSII), measured under actinic light exposure. Freezing sensitivity of F_V/F_M in non-acclimated plants clearly separated *sex1-1* from Col-0 and *pgm*, revealing an LT_{50} F_V/F_M value of only −2.9°C (Figure 7a). Following acclimation, F_V/F_M in *sex1-1* was still more sensitive to freezing than in the other genotypes, but the deviation from *pgm* became smaller. A similar pattern was obtained for parameters of light exposed leaves (Figure 7b). As an example, steady-state quantum yield of non-acclimated *sex1-1* displayed an LT_{50}ΦPSII of −2.7°C but dropped to −4.6°C following acclimation. Overall, there was a good concordance of freezing tolerance measured by ion leakage and freezing tolerance measured by chlorophyll fluorescence.

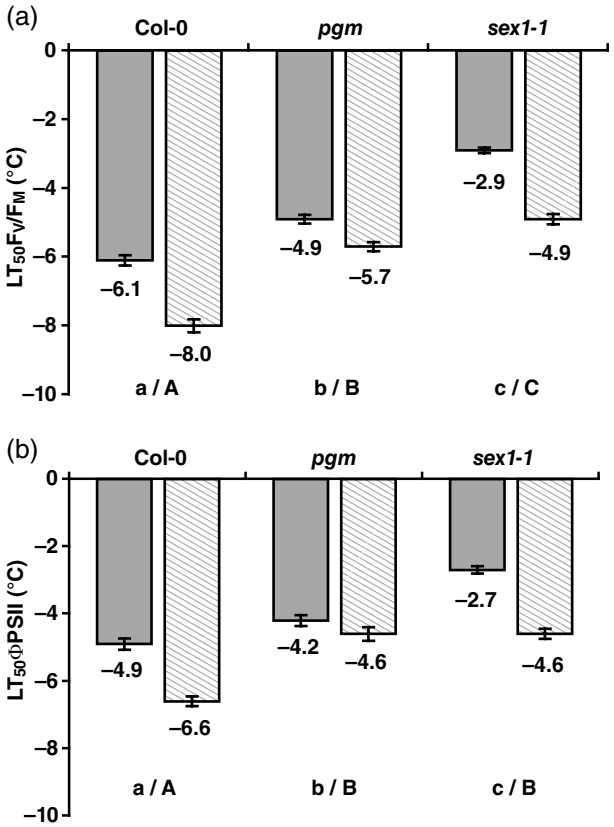

FIGURE 7 Freezing tolerance of electron transport in photosystem II in the genotypes Col-0, *pgm* and *sex1-1* before (grey bars) and after (hatched bars) cold acclimation. Temperatures of the half-maximal damage to (a) maximum quantum yield ($LT_{50}F_V/F_M$) and (b) actual quantum yield ($LT_{50}\Phi_{PSII}$) were calculated by non-linear regression of temperature series comprising 12 temperatures. Each sample consisted of three leaves from different plants. Error bars indicate 95% confidence intervals. Groups that do not share common letters are significantly different ($p < .05$, $n = 4$) within one treatment (lowercase for non-acclimated, uppercase for cold acclimated)

4 | DISCUSSION

4.1 | Pro and freezing tolerance

Elevated Pro levels have been detected in Arabidopsis mutants with elevated freezing tolerance, like the *eskimo-1* mutant (Xin & Browse, 1998) or transgenic plants overexpressing the cold-responsive transcription factor CBF3 (Gilmour, Sebolt, Salazar, Everard, & Thomashow, 2000). However, Pro levels could not be correlated with freezing tolerance in the present work. Here we found that the two P5CS mutants *p5cs2–1* and *p5cs1–4* showed the expected pattern of Pro reduction in the non-acclimated and acclimated state, respectively, but only the *p5cs2–1* mutant had reduced freezing tolerance in the non-acclimated state. Reduced proline content in cold-acclimated *p5cs1–4* mutants indicated that mainly P5CS1 mediates the accumulation of proline during cold stress, similar to other stress conditions. However, neither cold-acclimated *p5cs1–4* nor *p5cs2–1* mutants displayed altered freezing sensitivity. This is in agreement with earlier data that failed to show a correlation of Pro levels with acclimated freezing tolerance (Rohde, Hincha, & Heyer, 2004).

Interestingly, *p5cs2–1* showed substantial similarities to the *pgm* mutant. At ambient temperature, both mutants had reduced overall Pro levels, both had reduced freezing tolerance and both showed re-allocation of Pro to the vacuole, indicating substantial osmotic re-adjustment between cytoplasm and vacuole. The double-mutant *p5cs2–1*::*pgm* was indistinguishable from its parental lines with respect to proline allocation and freezing tolerance. In contrast, *pgm* and *p5cs2–1* plants were opposite for hexose levels at 22°C and deviated for sucrose and raffinose content. While both sugars and Pro are thought to be involved in cold acclimation, the similarity of non-acclimated *p5cs2–1*, *pgm* and *p5cs2–1*::*pgm* plants in Pro pattern and freezing tolerance, but not sugar levels, points to a role of Pro in non-acclimated freezing tolerance. At a cellular concentration of about 3 μmol $(g\ FW)^{-1}$, an osmoprotective function of Pro would have to be considered as marginal (Forlani et al., 2019). However, if 80% of Pro is in the cytosol of the wild type, and the cytosol is only 5% of cell volume (Winter, Robinson, & Heldt, 1993; Winter, Robinson, & Heldt, 1994), cytosolic Pro levels would reach about 50 μmol $(g\ FW)^{-1}$, which could make a substantial contribution to osmotic compensation during a freeze–thaw event. Other beneficial effects of Pro as compatible solute might also be more pronounced in the cytosol than in the vacuole. Thus, allocation of Pro mainly to the cytosol appears to be an important factor for non-acclimated freezing tolerance in Arabidopsis.

4.2 | Role of starch and soluble sugars in for freezing tolerance

Both, the *pgm* as well as the *sex1-1* mutants are disturbed in starch metabolism with the consequence of reduced diurnal starch turnover and insufficient carbohydrate availability during the night, which resulted in reduced growth rates of these mutants. The mutants with reduced starch degradation (*sex1-1* and *p5cs2–1*::*sex1-1*) had about 10-fold elevated starch levels at mid-day, when grown at 22°C. Sugar levels were more or less unchanged with the exception of raffinose depletion in the *pgm* genotypes. A contribution of low raffinose levels to low non-acclimated freezing tolerance is, however, unlikely, considering that raffinose levels are very low at ambient temperature and were so far not related to non-acclimated freezing tolerance (Knaupp et al., 2011). Hexose levels were reduced in non-acclimated *p5cs2–1* and *p5cs2*::*sex1-1* plants, which were also low in freezing tolerance. However, hexose levels were likewise reduced in acclimated *p5cs2–1* without an effect on freezing tolerance. A causal relation of low hexose levels and freezing sensitivity appears unlikely, considering that hexose levels are low in non-acclimated plants, preventing osmotic effects, and membrane protection by hexoses is marginal (Crowe, Oliver, Hoekstra, & Crowe, 1997).

It was reported that starch degradation via maltose formation is an important component of cold acclimation by protecting photosystem II in the chloroplast thylakoid membrane (Kaplan & Guy, 2005).

Freezing sensitivity of *pgm* could be enhanced because of the lack of maltose formation. However, maltose levels in *sex1-1* and *p5cs2–1*::*sex1-1* were about two-fold higher at ambient temperature and did not differ from wild type in the cold (Figure S2), yet both genotypes were highly freezing sensitive under both conditions. Yano et al. (2005) demonstrated that starch degradation in Arabidopsis rosettes was involved in enhancing freezing tolerance only at an early phase of acclimation, and *sex1* mutants resumed normal tolerance after 7 days in the cold. In contrast, we found reduced freezing tolerance before as well as 7 days after cold exposure of *sex1-1* plants. A striking difference between the two sets of experiments is the use of a day–night regime in our study. It has been demonstrated that such a treatment promotes starch build-up during the light phase (Caspar et al., 1985), and indeed, while Yano and co-workers found very little increase in starch content of *sex1-1*, we observed a more than 10-fold increase at ambient temperature and about six-fold in the cold. Thus, it could be assumed that the large amount of starch by itself may cause freezing sensitivity. Zeeman et al. (2002) demonstrated that starch granules in *sex1-1* mutants are larger than in wild-type plants and occupy more space in the chloroplast. There are several reports that large starch grains interfere with chloroplast function and may even cause disintegration of thylakoids (Sun, Li, & Liu, 2011). We analysed the influence of freeze–thaw stress on photosynthetic electron transport in *pgm* and *sex1-1* plants by chlorophyll fluorescence imaging. This revealed a particularly high freezing sensitivity of *sex1-1* chloroplasts, displaying LT_{50} values for maximum quantum yield ($LT_{50}F_V/F_M$) shifted to even higher temperatures than LT_{50} values determined by electrolyte leakage ($LT_{50}EL$). In contrast, $LT_{50}F_V/F_M$ was more negative than $LT_{50}EL$ in wild-type and *pgm* plants, which is in agreement with other reports for Arabidopsis (Knaupp et al., 2011). The reason for deleterious effects of starch grains on chloroplast function is unclear. Considering that starch grains in *sex1-1*, which occupy a large proportion of the plastids, are low in phosphate content, their water retention capacity is probably reduced. Thus, *sex1-1* chloroplasts may loose more water during freezing because their starch cannot bind water. In conclusion, reasons for freezing sensitivity of *pgm* and *sex1-1* seem to be different. Low Pro and its re-allocation from cytosol to vacuole appear to cause freezing sensitivity in *pgm*, whereas the high starch content in *sex1-1* plastids is a likely reason for its low freezing tolerance. This is supported by the non-additive effect of the *pgm*::*p5cs2–1* double mutation in contrast to the additive effect of *sex1-1*::*p5cs2–1* on freezing sensitivity.

ACKNOWLEDGMENTS

This work was supported by a grant from the Deutsche Forschungsgemeinschaft (DFG), grant Nr. HE-3087/10-2 to Arnd G. Heyer. We would like to thank Annika Allinger and Nadja Beuttenmüller for plant cultivation and the members of the Department of Plant Biotechnology for fruitful discussions.

CONFLICT OF INTEREST

Authors declare no conflict of interest.

AUTHOR CONTRIBUTION

Imke I. Hoermiller, Lilli Schönewolf and Henrik May conducted analytical experiments and analysed data, Dietmar Funck created mutant plants. Arnd G. Heyer and Dietmar Funck designed the study, all authors contributed to manuscript writing and approved the manuscript.

DATA AVAILABILITY STATEMENT

The data that support the findings of this study are available from the corresponding author upon reasonable request.

ORCID

Dietmar Funck https://orcid.org/0000-0002-9855-0419
Arnd G. Heyer https://orcid.org/0000-0003-2074-3234

REFERENCES

Altuntaş, C., Demiralay, M., Sezgin Muslu, A., & Terzi, R. (2020). Proline-stimulated signaling primarily targets the chlorophyll degradation pathway and photosynthesis associated processes to cope with short-term water deficit in maize. *Photosynthesis Research*, *144*, 35–48.

Büssis, D., & Heineke, D. (1998). Acclimation of potato plants to polyethylene glycol-induced water deficit - ii - contents and subcellular distribution of organic solutes. *Journal of Experimental Botany*, *49*, 1361–1370.

Caspar, T., Huber, S. C., & Somerville, C. (1985). Alterations in growth, photosynthesis, and respiration in a starchless mutant of *Arabidopsis thaliana* (L.) deficient in chloroplast phosphoglucomutase activity. *Plant Physiology*, *79*, 11–17.

Crowe, J., Oliver, A., Hoekstra, F., & Crowe, L. (1997). Stabilization of dry membranes by mixtures of hydroxyethyl starch and glucose - the role of vitrification. *Cryobiology*, *35*, 20–30.

de Mendiburu, F. (2016). Agricolae: Statistical procedures for agricultural research. R Package Version 1.2–4. Retrieved from https://CRAN.R-project.org/package=agricolae

Forlani, G., Trovato, M., Funck, D., & Signorelli, S. (2019). Regulation of proline accumulation and its molecular and physiological functions in stress defence. In M. A. Hossain, V. Kumar, D. J. Burritt, M. Fujita, & P. S. A. Mäkelä (Eds.), *Osmoprotectant-mediated abiotic stress tolerance in plants: Recent advances and future perspectives* (pp. 73–97). Cham: Springer International Publishing.

Funck, D., Baumgarten, L., Stift, M., von Wirén, N., & Schönemann, L. (2020). Differential contribution of P5CS isoforms to stress tolerance in Arabidopsis. *Frontiers in Plant Science*, *11*, 1483.

Funck, D., Stadelhofer, B., & Koch, W. (2008). Ornithine-δ-aminotransferase is essential for arginine catabolism but not for proline biosynthesis. *BMC Plant Biology*, *8*, 1–14.

Funck, D., Winter, G., Baumgarten, L., & Forlani, G. (2012). Requirement of proline synthesis during Arabidopsis reproductive development. *BMC Plant Biology*, *12*, 191.

Gilmour, S., Sebolt, A. M., Salazar, M. P., Everard, J. D., & Thomashow, M. (2000). Overexpression of the Arabidopsis CBF3 transcriptional activator mimics multiple biochemical changes associated with cold acclimation. *Plant Physiology*, *124*, 1854–1865.

Govrin, R., Obstbaum, T., & Sivan, U. (2019). Common source of cryoprotection and osmoprotection by osmolytes. *Journal of the American Chemical Society*, *141*, 13311–13314.

Hoermiller, I. I., Naegele, T., Augustin, H., Stutz, S., Weckwerth, W., & Heyer, A. G. (2017). Subcellular reprogramming of metabolism during cold acclimation in *Arabidopsis thaliana*. *Plant, Cell & Environment*, *40*, 602–610.

Kaplan, F., & Guy, C. L. (2005). RNA interference of Arabidopsis beta-amylase8 prevents maltose accumulation upon cold shock and

increases sensitivity of PSII photochemical efficiency to freezing stress. *The Plant Journal*, *44*, 730–743.
Knaupp, M., Mishra, K. B., Nedbal, L., & Heyer, A. G. (2011). Evidence for a role of raffinose in stabilizing photosystem II during freeze-thaw cycles. *Planta*, *234*, 477–486.
Maggio, A., Miyazaki, S., Veronese, P., Fujita, T., Ibeas, J. I., Damsz, B., … Bressan, R. A. (2002). Does proline accumulation play an active role in stress-induced growth reduction? *The Plant Journal*, *31*, 699–712.
Mattioli, R., Biancucci, M., El Shall, A., Mosca, L., Costantino, P., Funck, D., & Trovato, M. (2018). Proline synthesis in developing microspores is required for pollen development and fertility. *BMC Plant Biology*, *18*, 356.
Meena, M., Divyanshu, K., Kumar, S., Swapnil, P., Zehra, A., Shukla, V., … Upadhyay, R. S. (2019). Regulation of L-proline biosynthesis, signal transduction, transport, accumulation and its vital role in plants during variable environmental conditions. *Heliyon*, *5*, e02952.
Miller, G., Honig, A., Stein, H., Suzuki, N., Mittler, R., & Zilberstein, A. (2009). Unraveling Δ1-pyrroline-5-carboxylate-proline cycle in plants by uncoupled expression of proline oxidation enzymes. *The Journal of Biological Chemistry*, *284*, 26482–26492.
O'Leary, B. M., Oh, G. G. K., Lee, C. P., & Millar, A. H. (2019). Metabolite regulatory interactions control plant respiratory metabolism via target of rapamycin (TOR) kinase activation. *Plant Cell*, *32*, 666–682.
R Core Team. (2016). R: A language and environment for statistical computing. Retrieved from https://www.R-project.org/
Rasse, D. P., & Tocquin, P. (2006). Leaf carbohydrate controls over Arabidopsis growth and response to elevated CO2: An experimentally based model. *The New Phytologist*, *172*, 500–513.
Rienth, M., Romieu, C., Gregan, R., Walsh, C., Torregrosa, L., & Kelly, M. T. (2014). Validation and application of an improved method for the rapid determination of proline in grape berries. *Journal of Agricultural and Food Chemistry*, *62*, 3384–3389.
Ritz, C., Baty, F., Streibig, J. C., & Gerhard, D. (2015). Dose-response analysis using R. *PLoS One*, *10*, e0146021.
Rohde, P., Hincha, D., & Heyer, A. (2004). Heterosis in the freezing tolerance of crosses between two *Arabidopsis thaliana* accessions (Columbia-0 and C24) that show differences in non-acclimated and acclimated freezing tolerance. *The Plant Journal*, *38*, 790–799.
Rydeen, A. E., Brustad, E. M., & Pielak, G. J. (2018). Osmolytes and protein-protein interactions. *Journal of the American Chemical Society*, *140*, 7441–7444.
Sharma, S., Joji Grace Villamor, J., & Verslues, P. E. (2011). Essential role of tissue-specific proline synthesis and catabolism in growth and redox balance at low water potential. *Plant Physiology*, *157*(1), 292–304.
Sun, Z. P., Li, T. L., & Liu, Y. L. (2011). Effects of elevated CO2 applied to potato roots on the anatomy and ultrastructure of leaves. *Biologia Plantarum*, *55*, 675.
Szabados, L., & Savouré, A. (2010). Proline: A multifunctional amino acid. *Trends in Plant Science*, *15*, 89–97.
Székely, G., Ábrahám, E., Cséplő, Á., Rigó, G., Zsigmond, L., Csiszár, J., … Szabados, L. (2008). Duplicated P5CS genes of Arabidopsis play distinct roles in stress regulation and developmental control of proline biosynthesis. *The Plant Journal*, *53*, 11–28.
van den Boogaart, K. G., & Tolosana-Delgado, R. (2008). "Compositions": A unified R package to analyze compositional data. *Computational Geosciences*, *34*, 320–338.
Verbruggen, N., & Hermans, C. (2008). Proline accumulation in plants: A review. *Amino Acids*, *35*, 753–759.
Winter, H., Robinson, D. G., & Heldt, H. W. (1993). Subcellular volumes and metabolite concentrations in barley leaves. *Planta*, *191*, 180–190.
Winter, H., Robinson, D. G., & Heldt, H. W. (1994). Subcellular volumes and metabolite concentrations in spinach leaves. *Planta*, *193*, 530–535.
Xin, Z., & Browse, J. (1998). eskimo1 mutants of Arabidopsis are constitutively freezing-tolerant. *Proceedings of the National Academy of Sciences of the United States of America*, *95*, 7799–7804.
Xin, Z., & Browse, J. (2000). Cold comfort farm: The acclimation of plants to freezing temperatures. *Plant, Cell & Environment*, *23*, 893–902.
Yano, R., Nakamura, M., Yoneyama, T., & Nishida, I. (2005). Starch-related α-glucan/water dikinase is involved in the cold-induced development of freezing tolerance in Arabidopsis. *Plant Physiology*, *138*, 837–846.
Yu, T.-S., Kofler, H., Häusler, R. E., Hille, D., Flügge, U.-I., Zeeman, S. C., … Weber, A. (2001). The Arabidopsis sex1 mutant is defective in the R1 protein, a general regulator of starch degradation in plants, and not in the chloroplast hexose transporter. *Plant Cell*, *13*, 1907–1918.
Zeeman, S. C., Tiessen, A., Pilling, E., Kato, K. L., Donald, A. M., & Smith, A. M. (2002). Starch synthesis in Arabidopsis. Granule synthesis, composition, and structure. *Plant Physiology*, *129*, 516.

SUPPORTING INFORMATION

Additional supporting information may be found in the online version of the article at the publisher's website.

How to cite this article: Hoermiller, I. I., Funck, D., Schönewolf, L., May, H., & Heyer, A. G. (2022). Cytosolic proline is required for basal freezing tolerance in Arabidopsis. *Plant, Cell & Environment*, 45, 147–155. https://doi.org/10.1111/pce.14196